Active participation of CCR5+CD8+ T lymphocytes in the pathogenesis of liver injury in graft-versus-host disease

Masako Murai, … , Hitoshi Asakura, Kouji Matsushima

Article

We examined the molecular pathogenesis of graft-versus-host disease–associated (GVHD-associated) liver injury in mice, focusing on the role of chemokines. At the second week after cell transfer in the parent-into-F1 model of GVHD, CD8+ T cells — especially donor-derived CD8+ T cells — infiltrated the liver, causing both portal hepatitis and nonsuppurative destructive cholangitis (NSDC). These migrating cells expressed CCR5. Moreover, macrophage inflammatory protein-1α (MIP-1α), one of the ligands for CCR5, was selectively expressed on intralobular bile duct epithelial cells, endothelial cells, and infiltrating macrophages and lymphocytes. Administration of anti-CCR5 antibody dramatically reduced the infiltration of CCR5+CD8+ T lymphocytes into the liver, and consequently protected against liver damage in GVHD. The levels of Fas ligand (FasL) mRNA expression in the liver were also decreased by anti-CCR5 antibody treatment. Anti–MIP-1α antibody treatment also reduced liver injury. These results suggest that MIP-1α–induced migration of CCR5-expressing CD8+ T cells into the portal areas of the liver plays a significant role in causing liver injury in GVHD; thus, CCR5 and its ligand may be the novel target molecules of therapeutic intervention of hepatic GVHD.

Find the latest version:

https://jci.me/6642/pdf

Active participation of CCR5+CD8+ T lymphocytes in the pathogenesis of liver injury in graft-versus-host disease

Masako Murai,[1,2] Hiroyuki Yoneyama,[1,2] Akihisa Harada,[1] Zhang Yi,[1] Christian Vestergaard,[1] Baoyu Guo,[3] Kenji Suzuki,[2] Hitoshi Asakura,[2] and Kouji Matsushima[1]

[1]Department of Molecular Preventive Medicine and CREST, School of Medicine, The University of Tokyo, Tokyo 113-0033, Japan
[2]Third Department of Internal Medicine, Niigata University School of Medicine, Niigata 951, Japan
[3]Department of Molecular Pharmacology, Cancer Research Institute, Kanazawa University, Kanazawa 920, Japan

Address correspondence to: Kouji Matsushima, Department of Molecular Preventive Medicine, School of Medicine, The University of Tokyo, 7-3-1 Hongo, Bunkyo-ku, Tokyo 113-0033, Japan. Phone: 81-3-5841-3431; Fax: 81-3-5684-2297; E-mail: koujim@m.u-tokyo.ac.jp.

We examined the molecular pathogenesis of graft-versus-host disease–associated (GVHD-associated) liver injury in mice, focusing on the role of chemokines. At the second week after cell transfer in the parent-into-F1 model of GVHD, CD8+ T cells — especially donor-derived CD8+ T cells — infiltrated the liver, causing both portal hepatitis and nonsuppurative destructive cholangitis (NSDC). These migrating cells expressed CCR5. Moreover, macrophage inflammatory protein-1α (MIP-1α), one of the ligands for CCR5, was selectively expressed on intralobular bile duct epithelial cells, endothelial cells, and infiltrating macrophages and lymphocytes. Administration of anti-CCR5 antibody dramatically reduced the infiltration of CCR5+CD8+ T lymphocytes into the liver, and consequently protected against liver damage in GVHD. The levels of Fas ligand (FasL) mRNA expression in the liver were also decreased by anti-CCR5 antibody treatment. Anti–MIP-1α antibody treatment also reduced liver injury. These results suggest that MIP-1α–induced migration of CCR5-expressing CD8+ T cells into the portal areas of the liver plays a significant role in causing liver injury in GVHD; thus, CCR5 and its ligand may be the novel target molecules of therapeutic intervention of hepatic GVHD.

J. Clin. Invest. **104**:49–57 (1999).

Introduction

Graft-versus-host disease (GVHD) is one of the major complications of allogeneic bone marrow transplantation and blood transfusion (1). GVHD is initiated by donor T cells specific against the host antigens (1–3). Acute GVHD is a rapidly progressing systemic illness characterized by immunosuppression and tissue injury in various organs, including liver, skin, and intestinal mucosa (1–7). Especially in the liver, GVHD is characterized by portal hepatitis, nonsuppurative destructive cholangitis (NSDC), cholestasis, and endotheliitis (1, 2, 8). Although the molecular pathogenesis of GVHD remains to be uncovered, there is general agreement that infiltrating T lymphocytes play a central role (3–5, 7, 9, 10).

Previous studies have shown that in parent-into-F1 models, acute GVHD is characterized by a severe reduction in host lymphocytes and a profound immunodeficiency due to the activation of both donor CD4+ and CD8+ T cell subsets in response to host alloantigens (3, 11, 12). Early events that favor the development of acute GVHD are engraftment of CD8+ T cells and production of IFN-γ by donor CD4+ T cells (3, 12). However, these studies were carried out in the spleen, not in main target organs such as liver, skin, and intestine. In addition, recent studies suggest that both perforin- and Fas-mediated pathways are involved in the systemic signs of GVHD, and epithelial cell injury in liver, skin, and intestine appears to be Fas-mediated (4–6, 9, 10).These observations led us to investigate the main target organ, the liver, which has a pivotal role in maintaining homeostasis.

Leukocyte migration is a multistep process involving the sequential activation of various adhesion molecules located on the immune cells and the vascular endothelium, as well as a vast array of chemo-kines and their receptors (13–17). The involvement of chemokines and their receptors in inflammation has been elucidated during the last several years (18–23), but their functional roles in the progression of various diseases are not yet fully understood. In light of the recruitment of alloreactive T lymphocytes to a specific tissue site in GVHD, we focused on the characterization of chemokine receptors on these key lymphocytes and investigated the role of these cells in the pathogenesis of liver injury in a murine GVHD model.

Methods

Animals. C57BL/6 mice (B6, H-2b) were used as donors, and (B6 × DBA/2)F1 mice (BDF1, H-2b×d) were used as

allograft recipients; all mice were 8–12 weeks old at the time of the initial injection. BDF1 isografts were used as controls. All mice were purchased from Charles River Japan (Atsugi, Kanagawa, Japan). The mice were maintained in a pathogen-free mouse facility at The Department of Molecular Preventive Medicine of The University of Tokyo. All experiments conformed with approved animal care protocols of The University of Tokyo.

Preparation of recombinant GST protein fused with the NH$_2$-terminal portion of CCR5. We obtained cDNA encoding the NH$_2$-terminal extracellular portion of CCR5 by PCR, using the full-length cDNA strand and a set of oligonucleotides (5′-GCGAATTCATG-GATTTT-3′ and 5′-GCGGATCCAGCCGCAATTTG-3′) as a template and primers (24). The resulting fragment was digested with *Eco*RI and *Bam*HI and subcloned into a GST fusion protein expression vector, pGEM4T-3, which was predigested with *Eco*RI and *Bam*HI. Expression and purification of the GST fusion protein was performed as described previously (24).

Preparation of polyclonal antibodies against GST protein with the NH$_2$-terminal portion of CCR5. Two New Zealand white rabbits were immunized with 100 μg of the GST fusion protein in CFA (Iatron, Tokyo, Japan), 8 times at biweekly intervals. One week after the final immunization, rabbits were bled and sera were obtained and fractionated into IgG using a column packed with protein A-agarose (Pharmacia Biotech AB, Uppsala, Sweden). A portion of the IgG fraction was further digested with pepsin (Sigma Chemical Co., St. Louis, Missouri, USA), and the (Fab′)$_2$ fragment was obtained by sequential chromatographies using protein-A affinity and gel filtration columns as described previously (24). The anti-CCR5 antibody stained only CCR5 transfectants, not CXCR1 or CXCR2 transfectants, establishing binding specificity. Furthermore, the chemotaxis of liver mononuclear cells, which was induced by 100 ng/mL MIP-1α, was 50% inhibited by 100 μg/mL of IgG-fractionated anti-CCR5 antibody.

Induction of GVHD. Donor B6 spleen cells were prepared as described previously (25, 26). Briefly, 5×10^7 spleen cells harvested from C57BL/6 donors were injected into the tail veins of recipient mice. For the indicated experiments, 200 μg of anti-CCR5 antibody, rabbit γ globulin (Leinco, Ballwin, Missouri, USA), goat anti-mouse MIP-1α–neutralizing antibody (R&D Systems Inc., Minneapolis, Minnesota, USA), or goat γ globulin (Leinco Technologies Inc.) was dissolved in 200 μL of PBS. These were administered intravenously to mice the first week after cell transfer. At the first or second week after induction of GVHD, at least 3 mice were sacrificed. Approximately 1 mL of blood was obtained by cardiac puncture under ether anesthesia, and liver samples were collected.

Biochemical analysis. Blood samples were collected at the first week and the second week after grafting. Serum alanine transferase (ALT) levels were determined with a Fuji DRY-CHEM 5500V (Fuji Medical Systems, Tokyo, Japan) according to the manufacturer's instructions.

Histopathology. Tissues were fixed in 10% buffered formalin and embedded in paraffin. Sections were stained with hematoxylin and eosin and examined by light microscopy.

Preparation of liver-infiltrating lymphocytes. Mouse hepatic mononuclear cells were prepared as described previously (21). Briefly, the livers were pressed through stainless steel mesh and suspended in 10% FCS-DMEM. The cell suspensions were treated with 33% Percoll containing 100 U/mL heparin and were centrifuged at 800 *g* for 10 minutes at room temperature. The pellets were resuspended in RBC lysis solution, washed 3 times in DMEM, and resuspended in 10% FCS-DMEM.

Flow cytometry. Flow cytometric immunofluorescence analyses were performed as described previously (21). After incubation with anti-murine Fcγ receptor mAb 2.4G2 (PharMingen, San Diego, California, USA) for 10 minutes, cells were stained with saturating concentrations of FITC-, biotin-, or PE-conjugated mAb against CD3, CD4, CD8, B220, and H-2D^d (purchased from PharMingen unless otherwise indicated), and also stained with 10 μg/mL of rabbit anti-CCR5 polyclonal antibody. The instrument compensation was set in each experiment using single color–stained samples, and both CD4$^+$ T cells and CD8$^+$ T cells were sorted as described previously with an EPICS Elite cell sorter (Coulter Electronics Ltd., Hialeah, Florida, USA) (21).

Immunohistochemistry. The preparation of liver specimens was performed as described previously (21). Briefly, after removal, liver samples were fixed in periodate-lysine-paraformaldehyde, washed with PBS containing sucrose, embedded in Tissue-Tek OCT compound (Miles Inc., Elkhart, Indiana, USA), frozen in liquid nitrogen, and cut into 7-μm sections with a cryostat. After inhibition of endogenous peroxidase activity (21), the sections were incubated with a rabbit anti CCR5 antibody or control rabbit IgG at a concentration of 10 μg/mL. MIP-1α protein was detected with goat IgG antibody against recombinant mouse MIP-1α (R&D Systems Inc.) at a concentration of 10 μg/mL. CD4 and CD8 protein were identified with antibodies against CD4 and CD8, (PharMingen) respectively. They were treated sequentially with horseradish peroxidase–conjugated anti-rabbit IgG, horseradish peroxidase–conjugated anti-goat IgG (Southern Biotechnology Associates, Birmingham, Alabama, USA), or alkaline phosphatase–conjugated anti-rat IgG (Jackson Immuno-Research Laboratories Inc., West Grove, Pennsylvania, USA). After staining with 3,3′-diaminobenzidine (Wako Pure Chemical Industries Ltd., Osaka, Japan) or Vector Red Substrate Kit I (Vector Laboratories, Burlingame, California, USA), slides were counterstained with Mayer's hematoxylin.

Quantitative RT-PCR. Total RNA was isolated from liver specimens and sorted liver-infiltrating CD4$^+$ and CD8$^+$ T cells using RNAzol B (Tel-Test Inc., Friends-
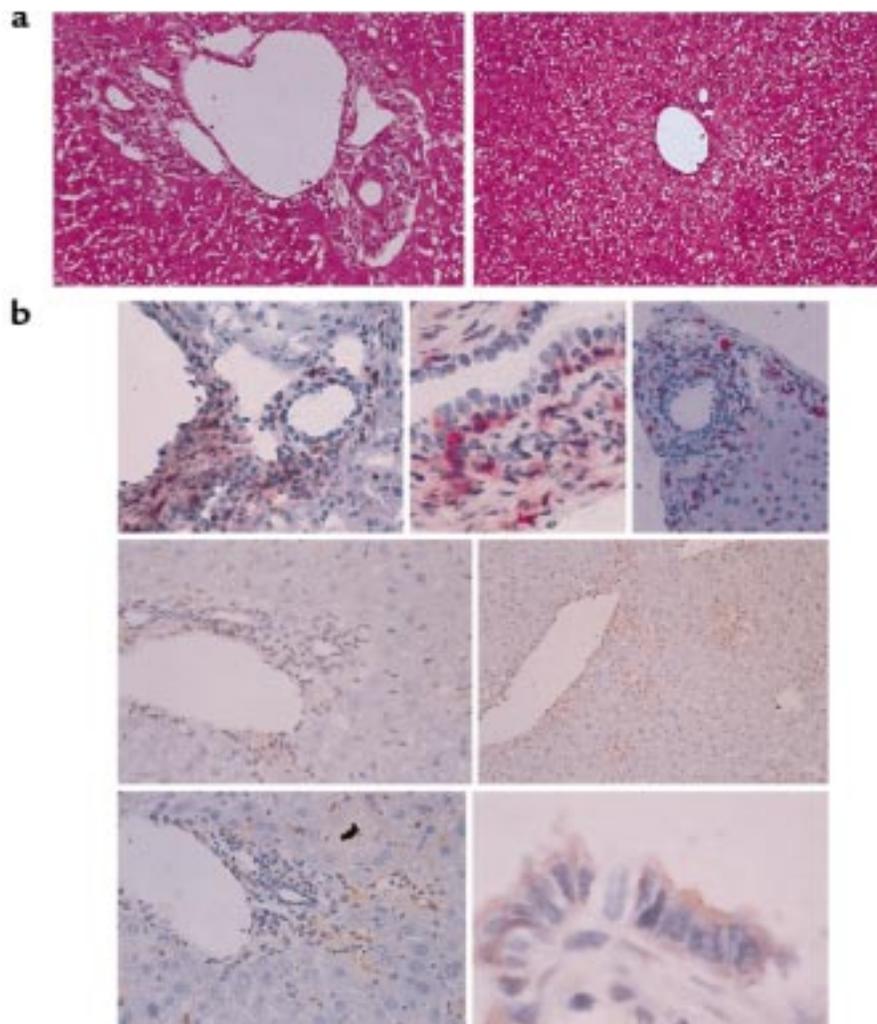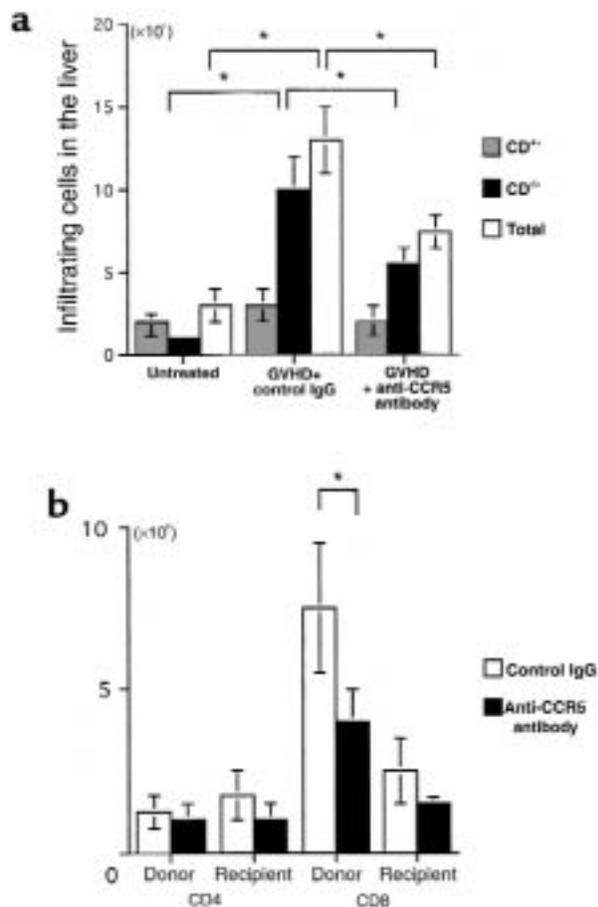
Figure 1
(**a**) Light-micrographic analysis of liver tissues. Histopathological examination was performed using hematoxylin and eosin–stained liver tissues obtained from GVHD-induced mice treated with control IgG (left) or anti-CCR5 antibody (right) at the second week after cell transfer. ×200. (**b**) Characterization of liver inflammatory foci during GVHD. GVHD-induced mouse livers were harvested and tissue sections prepared at the second week after induction. All micrographs show immunohistochemically stained frozen sections of areas encompassing a portal vein. Top row: left, CD8 staining, ×100; center, CD8 staining, ×400; right, CD4 staining, ×100. Center row: CCR5 staining, ×100. Bottom row: left, MIP-1a staining, ×100; right, MIP-1a staining, ×600. CD8 and CD4 are stained with red precipitates; CCR5 and MIP-1a are stained with brown precipitates.

wood, Texas, USA), according to the manufacturer's instructions. It was then reverse transcribed into cDNA and amplified. The expression of MIP-1α, MIP-1β, RANTES, CCR1, CCR4, CCR5, CXCR3, and Fas ligand (FasL) was determined by real-time quantitative PCR using the ABI7700 sequence detector system (Perkin-Elmer Applied Biosystems, Foster City, California, USA) (21, 22). The sense primer for MIP-1α was 5′-AAGGATACAAGCAGCAGCGAGTA-3′, and the antisense primer was 5′-TGCAGAGTGTCATGGTACAGAGAA-3′. The MIP-1α fluorescence-labeled probe was 5′-ACATCATGAAGGTCTCCACCACT-GCC-3′. The sense primer for MIP-1β was 5′-GATGGATTACTATGAGACCAGCAGT-3′, and the antisense primer was 5′-CAACTCCAAGTCACTCATGTACTCAG-3′. The MIP-1β fluorescence-labeled probe

was 5′-TGCTCCAAGCCAGCTGTGGTATTCCT-3′. The sense primer for RANTES was 5′-CATATG-GCTCGGACACCACT-3′, and the antisense primer was 5′-ACACACTTGGCGGTTCCTTC-3′. The RANTES fluorescence-labeled probe was 5′-CAAGTGCTC-CAATCTTGCAGTCGTG-3′. Primers and probes for CCR1, CCR4, CCR5, CXCR3, and FasL were described previously (21). The PCR products were also examined by 1.8% agarose gel electrophoresis. After ethidium bromide staining, bands were visible only at the expected size for each mRNA product.

Statistical analysis. Results are expressed as the mean ± SD. Unless otherwise indicated, statistical significance analyses were performed by 2-way ANOVA, with multiple comparison methods by Scheffe. $P < 0.05$ was accepted as statistically significant.

Figure 2

Effect of anti-CCR5 antibody on intrahepatic infiltration of mononuclear cells. (**a**) The number of CD4+ (dotted bars) and CD8+ (filled bars) T cells was determined by multiplying the total leukocyte number (open bars) by the fractions representing the CD4+ and CD8+ populations. Liver-infiltrating leukocytes were prepared from untreated mice and GVHD-induced mice treated with either control antibody or anti-CCR5 antibody. (**b**) Effect of anti-CCR5 antibody on the chimerism at the second week after induction. The number of donor-derived cells and recipient-derived cells was determined by multiplying the total leukocyte number by the fractions representing the H-2Dd–negative and H-2Dd–positive populations, respectively. Moreover, by multiplying the donor cell number and the recipient cell number by the fraction of CD4+ and CD8+ cells, the chimerism was determined in the GVHD-induced mice. Open bars: control antibody; filled bars: anti-CCR5 antibody. The mean ± SD of 6 mice is shown here. Five independent experiments were performed. *$P < 0.05$.

Results

Histopathological studies. Infiltration of mononuclear cells was not observed in either the untreated or the isografted livers (data not shown). In contrast, mononuclear cell infiltration was observed around the portal areas of the livers of BDF1 mice at the second week after infusion with B6 spleen cells. These cells were mainly lymphocytes, as determined by morphology. Infiltration of lymphocytes was often remarkable, although primarily confined to the portal areas. Occasionally they extended through the limiting plate into the liver lob-

ules. Intracanalicular bile stasis was also present. In many bile ducts, lymphocyte infiltration and epithelial disruption were observed (Figure 1a, left).

Engraftment of donor CD8+ T cells. To determine the total number of migrating leukocytes and the proportion of each type, liver leukocytes were isolated at different time points of the GVHD response, and flow cytometric analysis was performed. In isografted livers, both the total cell number and the ratio of CD4+ cells to CD8+ cells were almost the same as found in untreated livers (data not shown). During the second week of acute GVHD development, the total number of leukocytes in the liver was markedly increased, from 3.3×10^6 per liver to 1.3×10^7 per liver (Figure 2a).

To evaluate the contribution of T cells in the development of lesions, we analyzed cell surface expression of CD3, CD4, and CD8 using a flow cytometer. Intrahepatic lymphocytes were predominantly CD8+ T cells. The total number of CD8+ T cells increased from 10^6 per liver of untreated mice to 10^7 per liver of GVHD-induced mice at the second week. Few B cells were detected (data not shown). Furthermore, the number of cells of host origin in the liver that expressed the H-2Dd haplotype was also determined. Cells in the recipient that did not express H-2Dd were considered to be derived from the donor. Figure 2b shows that most liver-infiltrating CD8+ cells are H-2Dd negative (donor derived).

CCR5 expression on liver-infiltrating CD8+ T cells. Chemokine receptor expression on sorted liver-infiltrating cells was analyzed. Total liver T-cell RNA was extracted immediately after sorting, and real-time quantitative PCR was performed. At the first week after injection, liver CD8+ T cells predominantly expressed CCR1, CCR4, and CXCR3 mRNA (Figure 3a), whereas CCR2 and CCR7 mRNA was barely expressed (data not shown). The expression levels of CCR1, CCR4, and CXCR3 reached a peak at the first week after cell transfer and decreased during the second week after injection (Figure 3a). In contrast, CD8+ T cells expressed significantly more CCR5 mRNA at the second week of hepatic GVHD. Liver-infiltrating CD4+ T cells also expressed CCR5 mRNA 2 weeks after injection (Figure 3b), but at a much lower level than did CD8+ T cells.

To evaluate the presence and location of CD4+ T cells, CD8+ T cells, and CCR5-expressing cells in the GVHD-induced liver, immunohistochemical studies with antibodies directed against CD4, CD8, and CCR5 were carried out. On the second week after injection, there were dramatic increases in CD8+ cells per defined liver area in the mice (Figure 1b, top left and top center). CD4+ cells also infiltrated into the tissue surrounding portal areas (Figure 1b, top right).

In the livers of normal mice, there were a small number of CCR5-positive cells scattered throughout the liver parenchyma (data not shown). At the second week after cell transfer, CCR5 protein was detected in sinusoidal regions and in the lymphocytes infiltrating around portal areas (Figure 1b, center row). CD8+ and CCR5+ cell accumulation sites were associated with points of
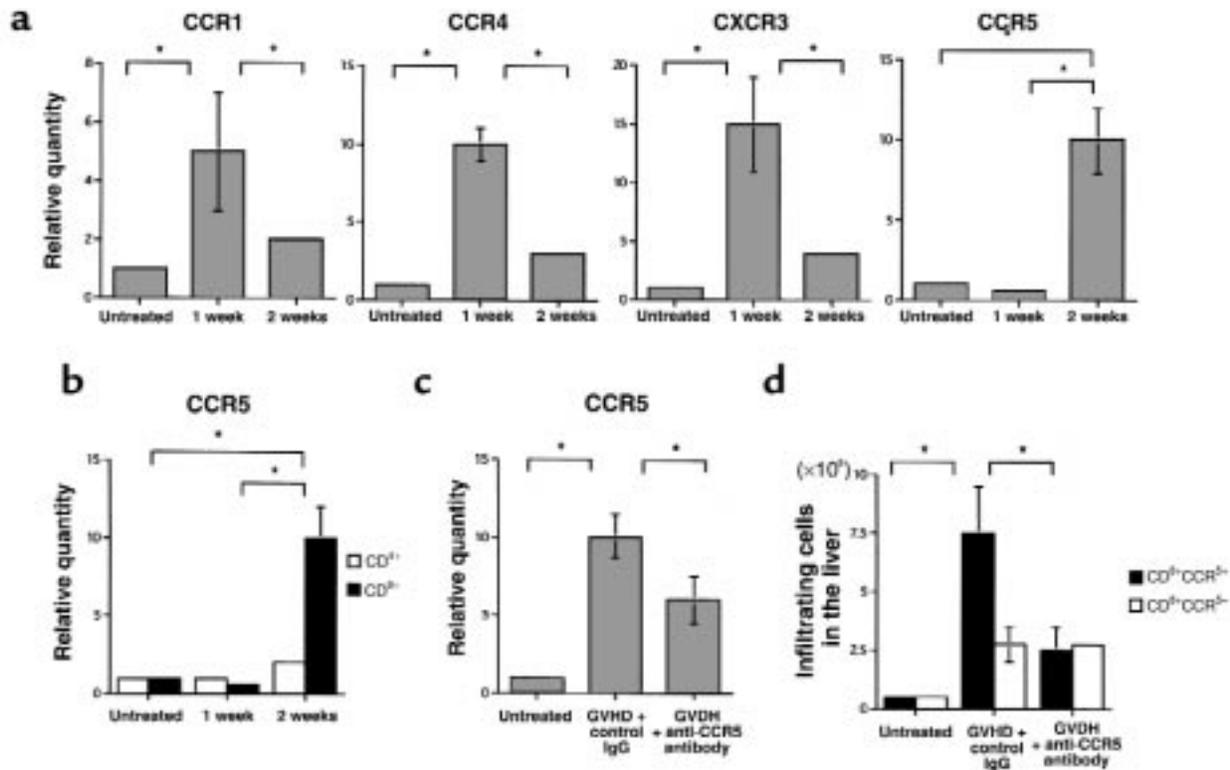
Figure 3

(**a**) Kinetics of CCR1, CCR4, CXCR3, and CCR5 mRNA expression in liver CD8+ T cells. Sorted liver CD8+ T cells were prepared from untreated and GVHD-induced mice during the 2 weeks after parental cell transfer. The amounts of CCR1, CCR4, CXCR3, and CCR5 were normalized to the level of GAPDH at each time point. Each normalized chemokine receptor value from untreated liver-infiltrating leukocytes was designated as the calibrator, and final relative quantity of mRNA was expressed relative to the calibrator. PCR was performed in triplicate for each experiment. (**b**) Kinetics of CCR5 mRNA expression in liver CD4+ and CD8+ T cells. Sorted liver CD4+ (open bars) and CD8+ (filled bars) T cells were prepared from untreated and GVHD-induced mice during the 2 weeks after parental cell transfer. (**c**) Effect of anti-CCR5 antibody on CD8+ T cells in the liver. Relative quantity of CCR5 mRNA of sorted liver CD8+ T cells prepared from untreated mice and GVHD-induced mice treated with either anti-CCR5 antibody or control antibody, at the second week after induction. (**d**) The number of CCR5+CD8+ T cells (filled bars) and CCR5−CD8+ T cells (open bars) was determined by multiplying the total leukocyte number by the fraction of CD3+, CD8+, and CCR5+ cells and totaling the results. Liver-infiltrating leukocytes were prepared from untreated mice and GVHD-induced mice treated with either anti-CCR5 antibody or control antibody, at the second week after induction. For each graph, data represent the mean ± SD of 6 mice. Each graph is representative of the results obtained from 3 independent experiments. *$P < 0.05$.

NSDC (Figure 1b, top left and center left). In contrast to CD4+ cells, CD8+ cells migrated into the sinusoids as well as the tissues surrounding portal areas. Moreover, CD8+ T cells invading the bile duct epithelial cells were observed (Figure 1b, top center). These results suggest that it is primarily CCR5-expressing CD8+ T cells that migrate into the liver at the second week after injection, and that these cells may induce hepatic GVHD. However, involvement of the small numbers of CD4+ or host-derived CD8+ T lymphocytes in the pathogenesis of GVHD could not be ruled out.

Anti-CCR5 antibody reduces CD8+ T-cell infiltration into the liver. To investigate the role of CCR5-expressing cells in the pathogenesis of hepatic GVHD, 200 μg of neutralizing anti-CCR5 antibody was administered at the first week after cell transfer. In histological findings, mice treated with B6 spleen cells plus anti-CCR5 antibody showed less cellular infiltration and a lower frequency of NSDC lesions (Figure 1a, right) compared with con-

trol antibody–treated GVHD-induced mice (Figure 1a, left). The administration of anti-CCR5 antibody decreased the number of total infiltrating lymphocytes by ~21% (from 1.3×10^7 to 7.3×10^6 cells per liver). The number of infiltrating CD8+ T cells was also reduced, by 48% (from 10^7 to 5.2×10^6 cells per liver). In neither case was the number of cells reduced to the level seen in liver tissue from normal mice (Figure 2a). The number of donor CD8+ T cells was particularly reduced (Figure 2b). It is noteworthy that after anti-CCR5 antibody treatment, the expression level of CCR5 mRNA of intrahepatic CD8+ T cells was decreased (Figure 3c) and the number of CCR5+CD8+ T cells was selectively decreased (Figure 3d). In addition, serum ALT levels were monitored, as an indicator of liver damage (Figure 4a). The ALT level of isografted mice was almost indistinguishable from that of untreated mice. In allografted mice, serum ALT levels were increased by the end of the second week after injection. In contrast,

treatment with anti-CCR5 antibody led to a marked reduction of serum ALT levels compared with control antibody treatment.

FasL mRNA expression in the liver was also analyzed by real-time quantitative PCR (Figure 4b). FasL mRNA was faintly expressed in untreated and isografted livers, but was highly induced by injection of parent spleen cells after the second week. Anti-CCR5 antibody treatment significantly reduced FasL mRNA expression in allografted livers compared with control antibody treatment.

T-cell trafficking to liver depends largely on MIP-1α. To identify which chemokine was responsible for chemoattracting CCR5+CD8+ T cells, total RNA was prepared from the livers of untreated mice and GVHD-induced mice, and the mRNA expression of the ligands for CCR5, MIP-1α, MIP-1β, and RANTES was examined (Figure 5a). MIP-1α mRNA was not detectable in either the untreated or isografted control livers. However, MIP-1α mRNA was detected from the first week after cell transfer in GVHD-induced mice, and the expression levels were dramatically increased by the second week (Figure 5b). MIP-1β mRNA was barely expressed in both untreated and treated mice. RANTES mRNA was detected in small amounts in the livers of untreated and treated mice, and its expression level was almost constant.

Immunohistochemical studies were carried out with antibodies specific for MIP-1α to confirm the induction of MIP-1α protein and to identify the location of its production in the liver. There were no cells expressing MIP-1α in the untreated or isografted mice (data not shown). In contrast, significant levels of MIP-1α were expressed in the livers of GVHD-induced mice after the first week — particularly in macrophages, lymphocytes, and endothelial cells. Furthermore, MIP-1α was expressed on sinusoidal lining cells in the liver parenchyma and on the intralobular bile ducts in the portal areas (Figure 1b, bottom row). The control antibody did not stain the same tissue, indicating the specificity of the reaction (data not shown). The administration of anti–MIP-1α antibody decreased the number of total infiltrating lymphocytes and the total number of CD8+ T cells (Figure 5c), as well as serum ALT levels (Figure 5d). These results suggest that CCR5+CD8+ T cells were recruited to the liver by MIP-1α protein that was produced mainly by macrophages, lymphocytes, bile duct epithelial cells, and endothelial cells during GVHD.

Discussion

Hepatic GVHD is characterized by the development of portal hepatitis, endotheliitis, and the progression to NSDC. Expansion of the portal tracts by a cellular infiltration was one of the earliest abnormalities in this model, and occurred concomitantly with the appearance of transient acute liver failure (Figure 1a, left; Figure 4a). The inflammatory cell infiltration in the liver was composed of T lymphocytes and mononuclear phagocytes (Figure 1a, left). These cells are known to induce hepatic injury and bile duct destruction by a variety of mechanisms including the Fas-FasL pathway (4–7, 9, 10, 27)

and the CD40-CD40L pathway (28). However, how the migration of effector cells into the liver is regulated remains to be established.

This study demonstrates that the number of lymphocytes infiltrating the liver was increased in the second week after cell transfer, and that CD8+ T cells were the predominant infiltrating cells (Figure 2a). Interestingly, liver CD8+ T cells expressed higher levels of CCR5 mRNA than did liver CD4+ T cells (Figure 3b). In immunohistochemistry studies, CCR5-positive cells infiltrated the portal area and were scattered throughout the parenchyma (Figure 1b, center row). Also at the second week after cell transfer, portal hepatitis and NSDC were detected (Figure 1a, left). Administration of anti-CCR5 antibody restricted the migration of lymphocytes into the GVHD-induced livers (Figure 2a) and reduced the amount of histopathological damage
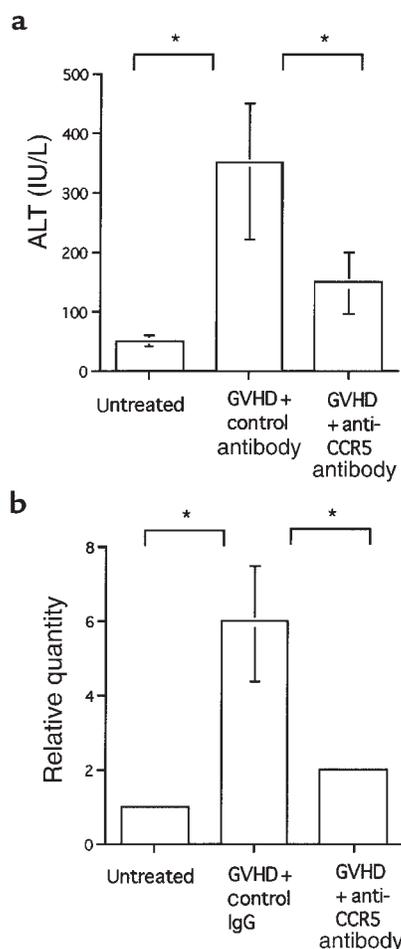
Figure 4

(**a**) Effect of anti-CCR5 antibody on serum ALT levels. The serum ALT levels of untreated mice and GVHD-induced mice treated with either anti-CCR5 antibody or control antibody, at the second week after induction. (**b**) Effect of anti-CCR5 antibody on FasL mRNA in the liver. Total RNA was isolated from liver tissue of untreated mice and GVHD-induced mice treated with either control antibody or anti-CCR5 antibody, at the second week after induction. The data represent the mean ± SD of 6 mice. Each graph is representative of the results obtained from 3 independent experiments. *$P < 0.05$.
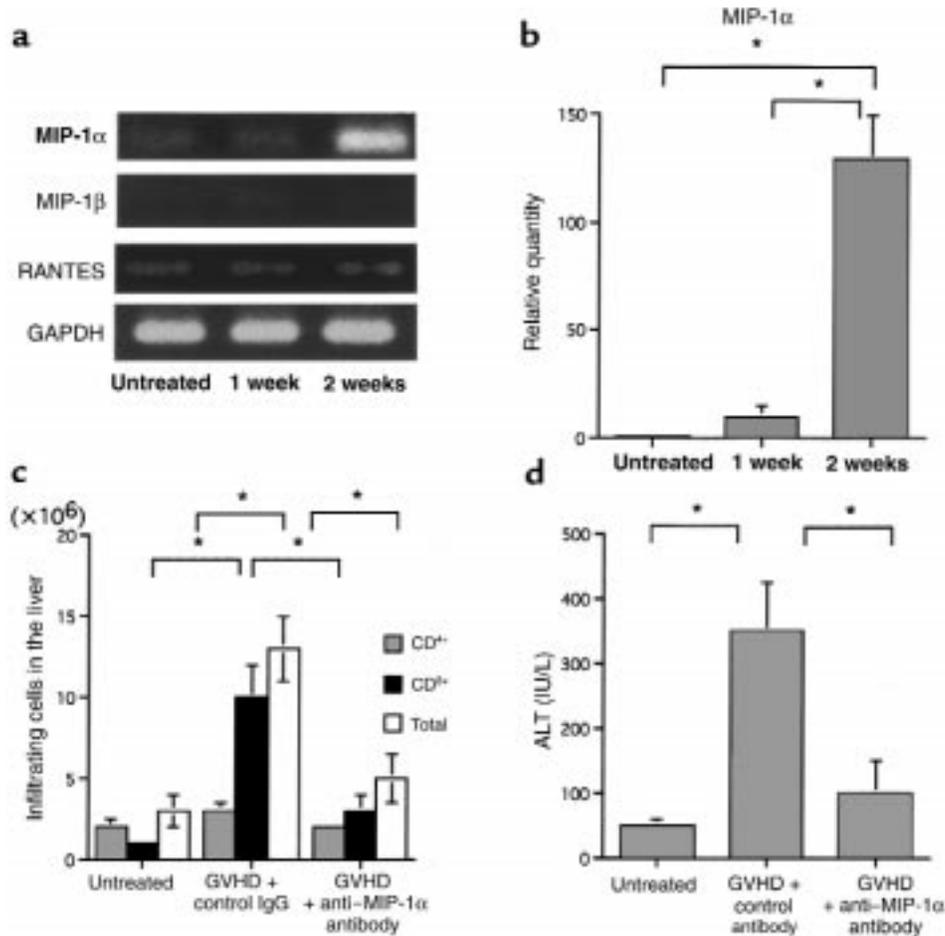
Figure 5
(**a**) Kinetics of MIP-1α, MIP-1β, and RANTES mRNA expression in the liver. Total RNA was isolated from liver tissues of untreated and GVHD-induced mice during the second week after induction. RT-PCR cDNA products were generated and amplified using oligonucleotide primers specific to MIP-1α, MIP-1β, RANTES, or the housekeeping gene GAPDH. (**b**) The amount of MIP-1α was normalized to the level of GAPDH at each time point. Each normalized MIP-1α value of untreated liver was designated as the calibrator, and final relative quantity of mRNA was expressed relative to the calibrator. PCR was performed in triplicate for each experiment. (**c**) Effect of anti–MIP-1α antibody on intrahepatic infiltration of mononuclear cells. The number of CD4+ (dotted bars) and CD8+ (filled bars) cells was determined by multiplying the total leukocyte number (open bars) by the fraction of CD4+ and CD8+ cells. Liver-infiltrating leukocytes were prepared from untreated mice and GVHD-induced mice treated with either control antibody or anti–MIP-1α antibody. (**d**) Effect of anti–MIP-1α on serum ALT levels. Shown are serum ALT levels of untreated mice and GVHD-induced mice treated with either control antibody or anti–MIP-1α antibody, at the second week after induction. The data represent the mean ± SD of 6 mice. Graph is representative of results obtained from 3 independent experiments. *P* < 0.05.

(Figure 1a, right). It also downregulated the expression level of CCR5 in both mRNA and protein of CD8+ T cells in the liver (Figure 3, c and d). These results suggest that the number of immunoreactive cells correlates directly with histopathological severity, and that these cells are mostly CCR5+CD8+ T cells.

The selective recruitment of leukocytes at inflammation and immune-response sites has been explained by the specific expression of chemokine receptors on each type of leukocyte (13, 15–23). The chemokine receptor CCR5 has been shown to be expressed on monocytes/macrophages and lymphocytes, especially Th1-type cells (18–20, 29). Moreover, expression and chemotactic migration of CCR5 depend on the activation of Th1 cells, in particular for IL-2, but not with anti-CD3 or anti-CD28 antibodies (18). However, the

precise mechanism of the regulation of CCR5 expression has not yet been explained. In our model, both CCR5 mRNA and protein were hardly detected in untreated mouse liver (data not shown). However, CCR5 was expressed in the liver at the peak of hepatic damage, primarily by CD8+ T cells. These results and those shown in Figure 3a (showing chemokine receptor mRNA expression by CD8+ T cells in liver after GVHD induction) suggest that the immunopathophysiology of hepatic GVHD can be divided into 2 phases: an inductive phase and an effector phase. In the inductive phase, inoculated donor cells recognize antigenic disparities expressed on recipient tissues, resulting in alloactivation and proliferation of the allogeneic donor T cells. In the effector phase, inflammatory reactions characterized by massive mononu-

clear cell infiltration and histopathological damage may develop in the host liver.

The mRNA level of MIP-1α, one of the ligands of CCR5, was gradually increased in GVHD-induced liver (Figure 5, a and b), and MIP-1α protein was detected in the lymphocytes, macrophages, endothelial cells, and bile duct epithelial cells in the infiltrated portal areas and sinusoids (Figure 1b, bottom row). Expression of mRNA by RANTES and MIP-1β, which are also ligands of CCR5, could be faintly detected in the GVHD-induced liver, but expression levels did not change during the course of disease (Figure 5a). Peak expression of mRNA by monokine induced by IFN-γ (Mig) and IFN-γ–inducible protein (IP-10), which are considered to be selective chemoattractants for activated T lymphocytes, was 1 week after injection; thereafter, expression levels gradually decreased. Secondary lymphoid tissue chemokine (SLC) and EBV-induced gene 1-ligand chemokine (ELC), which act on T cells, also showed peak mRNA expression 1 week after cell transfer (data not shown). The pattern of mRNA expression of these chemokines was similar to that of their receptors. Moreover, the administration of anti–MIP-1α antibody greatly reduced liver injury (Figure 5, c and d) . These results suggest that MIP-1α is the most influential factor among these studied chemokines for recruitment of CCR5^{+}CD8^{+} T lymphocytes into the liver. CCR5 is selectively induced in the effector phase, primarily on CD8^{+} T cells, and the migration of CCR5-expressing cells may depend on MIP-1α. It is possible that various chemokines not only chemoattract leukocytes into specific tissues but also modulate various functions of these cells in each phase; therefore, anti-CCR5 antibody treatment reduced liver injury as a result of the depletion of CCR5-expressing cells in the liver. Recently it has been reported that activated CD8^{+} T cells preferentially migrate in vitro in response to MIP-1α (30). Our data, taken from in vivo studies, agree with this result.

IFN-γ has been considered to play a critical role in the development of acute GVHD (8, 12, 31–37). However, a recent study, using a mouse IFN-γ gene knockout (GKO) transplant into a GKO mouse model, demonstrated that lethal acute GVHD can be induced in the complete absence of IFN-γ (36). Consistent with this, in our model, contrary to the reduction of liver injury by anti-CCR5 antibody treatment, IFN-γ production by liver-infiltrating T cells was unexpectedly upregulated (data not shown). Moreover, it has been reported that administration of exogenous IFN-γ markedly inhibits GVHD (8), and IFN-γ–inducing factor (IL-18) and IL-12 enhanced the FasL-mediated cytotoxicity of Th1 cells, whereas IFN-γ had no effect on GVHD (37). Therefore, the results of our own and other studies have shown that IFN-γ may not necessarily be critical for the pathogenesis of liver GVHD.

Recent investigations have revealed that, in spite of FasL upregulation on both donor CD4^{+} and CD8^{+} T cells in the parent-into-F1 model, all the anti-host

cytotoxic T lymphocyte (CTL) activity is accounted for by donor CD8^{+} CTL (4–6). Consistent with these studies, we found that after treatment with anti-CCR5 antibody, donor CD8^{+} T cells were selectively diminished and FasL mRNA expression was decreased in the liver (Figure 4b). Consequently, liver damage was reduced (Figure 1a, right; Figure 4a). Moreover, the ratio of CD4^{+} T cells and CD8^{+} T cells in the liver after anti-CCR5 antibody treatment was close to that in untreated liver (Figure 2a). These results suggest that FasL expression on CD8^{+} T cells contributes to liver damage in GVHD.

Our inability to achieve complete inhibition of both cell migration to liver and hepatic damage by anti-CCR5 antibody treatment suggests either failure to neutralize all CCR5-expressing cells in vivo or that other chemokine receptors may also contribute to the liver injury induced by GVHD. However, our studies indicate that chemokine receptors, especially CCR5 and its ligand MIP-1α, are significantly involved in the pathogenesis of liver injury in GVHD.

Overall, the data presented in this study demonstrate that CCR5-expressing CD8^{+} T cells recruited into liver trigger liver damage in our model. CCR5 and MIP-1α may be the target molecules for therapeutic intervention to prevent, as well as predict, GVHD. Thus, our findings provide a basis for the development of a new generation of drugs that protect liver function by antagonizing chemokine receptors in order to prevent harmful cells from migrating into the liver.

1. Ferrara, J.L.M., and Deeg, H.J. 1991. Graft-versus-host disease. *N. Engl. J. Med.* **324**:667–674.
2. Gleichmann, E., Pals, S.T., Rolink, A.G., Radaszkiewicz, T., and Gleichmann, H. 1984. Graft-versus-host reactions: clues to the ethiopathology of a spectrum of immunological diseases. *Immunol. Today.* **5**:324–332.
3. Rus, V., Svetic, A., Nguyen, P., Gause, W.C., and Via, C.S. 1995. Kinetics of Th1 and Th2 cytokine production during the early course of acute and chronic murine graft-versus-host disease. *J. Immunol.* **155**:2396–2406.
4. Bobe, P., et al. 1997. Fas-mediated liver damage in MRL hemopoietic chimeras undergoing lpr-mediated graft-versus-host disease. *J. Immunol.* **159**:4197–4204.
5. Baker, B.M.B., Altman, N., Podack, E., and Levy, R.B. 1996. The role of cell-mediated cytotoxicity in acute GVHD after MHC-matched allogeneic bone marrow transplantation in mice. *J. Exp. Med.* **183**:2645–2656.
6. Braun, M.Y., Lowin, B., French, L., Acha-Oreba, H., and Tschopp, J. 1996. Cytotoxic T cells deficient in both functional Fas ligand and perforin show residual cytolytic activity yet lose their capacity to induce lethal acute graft-versus-host disease. *J. Exp. Med.* **183**:657–661.
7. Williamson, E., Garside, P., Bradley, A., More, I.A.R., and Mowat, A.M. 1997. Neutralizing IL-12 during induction of murine acute graft-versus-host disease polarizes the cytokine profile toward a Th2-type alloimmune response and confers long term protection from disease. *J. Immunol.* **159**:1208–1215.
8. Brok, H.P.M., Heidt, P.J., Van der Meide, P.H., Zurcher, C., and Vossen, J.M. 1993. Interferon-gamma prevents graft-versus-host disease after allogeneic bone marrow transplantation in mice. *J. Immunol.* **151**:6451–6459.
9. Shustov, A., Nguyen, P., Finkelman, F., Elkon, K.B., and Via, C. S. 1998.

Differential expression of Fas and Fas ligand in acute and chronic graft-versus-host disease: up-regulation of Fas and Fas ligand requires CD8+ T cell activation and IFN-γ production. *J. Immunol.* **161**:2848–2855.

10. Via, S.C., Nguyen, P., Shustov, A., Drappa, J., and Elkon, K.B. 1996. A major role for the Fas pathway in acute graft-versus-host disease. *J. Immunol.* **157**:5387–5393.

11. Allen, D.R., Staley, T.A., and Sidman, C.L. 1993. Differential cytokine expression in acute and chronic murine graft-versus-host-disease. *Eur. J. Immunol.* **23**:333–337.

12. Ellison, C.A., Fischer, J.M.M., HayGlass, K.T., and Gartner, J.G. 1998. Murine graft-versus-host disease in an F1-hybrid model using IFN-γ gene knockout donors. *J. Immunol.* **161**:631–640.

13. Baggiolini, M. 1998. Chemokines and leukocyte traffic. *Nature.* **392**:565–568.

14. Butcher, E.C., and Picker, L.J. 1996. Lymphocyte homing and homeostasis. *Science.* **272**:60–66.

15. Littman, R.D. 1998. Chemokine receptors: keys to AIDS pathogenesis? *Cell.* **93**:677–680.

16. Rollins, J.B. 1997. Chemokines. *Blood.* **90**:909–928.

17. Farber, J.M. 1997. Mig and IP-10 chemokines that target lymphocytes. *J. Leukoc. Biol.* **61**:246–257.

18. Loetscher, P., et al. 1998. CCR5 is characteristic of Th1 lymphocytes. *Nature.* **391**:344–345.

19. Qin, S., et al. 1998. The chemokine receptors CXCR3 and CCR5 mark subsets of T cells associated with certain inflammatory reactions. *J. Clin. Invest.* **101**:746–754.

20. Rottman, J.B., et al. 1997. Cellular localization of the chemokine receptor CCR5. *Am. J. Pathol.* **151**:1341–1351.

21. Yoneyama, H., et al. 1998. Pivotal role of TARC, a CC chemokine, in bacteria-induced fulminant hepatic failure in mice. *J. Clin. Invest.* **102**:1933–1941.

22. Gibson, U.E.M, Heide, C.A., and Williams, P.M. 1996. A novel method for real time quantitative RT-PCR. *Genome Res.*, **6**:995–1001.

23. Zhou, Y., et al. 1998. Impaired macrophage function and enhanced T cell-dependent immune response in mice lacking CCR5, the mouse homologue of the major HIV-1 coreceptor. *J. Immunol.* **160**:4018–4025.

24. Su, S.-B., Mukaida, N., Wang, J.-B., Nomura, H., and Matsushima, K. 1996. Preparation of specific polyclonal antibodies to a C-C chemokine receptor, CCR1, and determination of CCR1 expression on various types of leukocytes. *J. Leukoc. Biol.* **60**:658–666.

25. Saitoh, T., et al. 1990. Depletion of CD8+ cells exacerbates organ-specific autoimmune diseases induced by CD4+ T cells in semiallogeneic hosts with MHC class II disparity. *J. Immunol.* **145**:3268–3275.

26. Suzuki, K., Narita, T., Yui, R., Asakura, H., and Fujiwara, M. 1994. Mechanism of the induction of autoimmune disease by graft-versus-host reaction. *Lab. Invest.* **70**:609–619.

27. Williamson, E., Garside, P., Bradley, J.A., and Mowat, A.M. 1996. IL-12 is a central mediator of acute graft-versus-host disease in mice. *J. Immunol.* **157**:689–699.

28. Saito, K., et al. 1998. Involvement of CD40 ligand-CD40 and CTLA4-B7 pathways in murine acute graft-versus-host disease induced by allogeneic T cells lacking CD28. *J. Immunol.* **160**:4225–4231.

29. Bonecchi, R., et al. 1998. Differential expression of chemokine receptors and chemotactic responsiveness of type 1 T helper cells (Th1s) and Th2s. *J. Exp. Med.* **187**:129–134.

30. Taub, D.D., Conlon, K., Lioyd, A.R., Oppenheim, J.J., and Kelvin, D.J. 1993. Preferential migration of activated CD4+ and CD8+ T cells in response to MIP-1α and MIP-1β. *Science.* **260**:355–358.

31. Fowler, D.H., Kurasawa, K., Husebekk, A., Cohen, P.A., and Gress, R.E. 1994. Cells of the Th2 cytokine phenotype prevent LPS-induced lethality during murine graft-versus-host reaction. *J. Immunol.* **152**:1004–1013.

32. Kreneger, W., Snyder, K.M., Byon, J.C.H., Falzarano, G., and Ferrara, J.L.M. 1995. Polarized type 2 alloreactive CD4+ and CD8+ donor T cells fail to induce experimental acute graft-versus-host disease. *J. Immunol.* **155**:585–593.

33. Liu, Y., and Janeway, C.A. 1990. Interferon-gamma plays a critical role in induced cell death of effector T cell: a possible third mechanism of self-tolerance. *J. Exp. Med.* **172**:1735–1739.

34. Novelli, F., et al. 1994. Environmental signals influencing expression of the IFN-γ receptor on human T cells control whether IFN-γ promotes proliferation or apoptosis. *J. Immunol.* **152**:496–504.

35. Novelli, F., et al. 1997. Expression and role in apoptosis of alpha- and beta-chains of the IFN-gamma receptor on human Th1 and Th2 clones. *J. Immunol.* **159**:206–213.

36. Yang, Y.-G., Dey, B.R., Sergio, J.J., Peason, D.A., and Sykes, M. 1998. Donor-derived interferon-γ is required for inhibition of acute graft-versus-host disease by interleukin 12. *J. Clin. Invest.* **102**:2126–2135.

37. Yang, Y.-G., et al. 1997. Interleukin-12 prevents the graft-versus-host leukemia effect of allogeneic CD8 T cells while inhibiting CD4-dependent graft-versus-host disease in mice. *Blood.* **90**:4651–4660.